Phenotypic evolution as an Ornstein-Uhlenbeck process: The effect of environmental variation and phenotypic plasticity

Clécio C. de Souza Silva, Diego Cirne, Osmar Freitas, and Paulo R. A. Campos*
Departamento de Física, Universidade Federal de Pernambuco, 50740-560 Recife-PE, Brazil

(Received 18 October 2022; accepted 13 February 2023; published 24 February 2023)

Here we investigate phenotypic evolution from the perspective of the Ornstein-Uhlenbeck (OU) process. Evolutionarily speaking, the model assumes the existence of stabilizing selection toward a phenotypic optimum. The standard (OU) model is modified to include environmental variation by taking a moving phenotypic optimum and endowing organisms with phenotypic plasticity. These two processes lead to an effective fitness landscape, which deforms the original. We observe that the simultaneous occurrence of environmental variation and phenotypic plasticity leads to skewed phenotypic distributions. The skewness of the resulting phenotypic distributions strongly depends on the rate of environmental variation and strength of selection. When generalized to more than one trait, the phenotypic distributions are not only affected by the magnitude of the rate of environmental variation but also by its direction. A remarkable feature of our predictions is the existence of an upper bound for the critical rate of environmental variation to allow population persistence, even if there is no cost associated with phenotypic plasticity.

DOI: 10.1103/PhysRevE.107.024417

I. INTRODUCTION

Over the past years, several events have influenced and shaped biodiversity on Earth, from geological climate responses [1] to human-induced habitat fragmentation [2]. Under environmental variation, species must adapt or migrate to suitable habitats. The pace of environmental change strongly determines the fate of populations. If unable to disperse, population declines or reaches extinction when the magnitude of environmental change pushes species beyond their ability to adapt [3].

The set of genomes comprising an organism determines their expressed traits as a genotype-phenotype map $\mathcal{G} \to \mathcal{P}$. Accordingly, the interaction of the phenotype with the environment determines the organism's fitness, i.e., its adaptation to the environment. To better adapt to varying environments, organisms may modify their traits between generations and thus improve their fitness. The modern synthesis assumes a one-way relationship between environment and adaptation in driving evolutionary changes in which the environment poses new challenges concerning the organism's ability to persist and the organism's propensity to generate new variants, mainly through mutations that occur randomly, irrespective of their consequences [4]. Accordingly, evolutionarily significant phenotypic variation arises from genetic mutations, which in its turn can face the changes posed by the environment. However, the time and tempo of environmental changes may take effect within an organism's lifetime, requiring a faster adaptation response than by genotypic evolution alone.

Contemporary evolutionary works acknowledge the role of developmental or phenotypic plasticity on evolutionary responses of natural populations when faced with environmental variation [5]. Phenotypic plasticity refers to the capacity of an organism to express different phenotypic states from the same genome in response to the environment [6,7]. Plastic response to environmental change can modulate the physiology, morphology, and behavior of individuals [8,9]. Evidence of phenotypic response abound, especially those related to temperature variation in the face of global warming [9,10]. These plastic responses bring about critical ecological consequences for species interactions and ecological communities [11]. A massive body of literature reports the well-documented effect of temperature on predator-prey and consumer-resource interactions, such as those verified for vertebrate and invertebrate predators on plant communities [12–14] and fish predators on phytoplankton biomass [15], to mention just a few.

In studying phenotypic evolution, important insights have been inferred from two analytical and tractable models: the Brownian motion (BM) and Ornstein-Uhlenbeck (OU). Both are classical stochastic models from statistical mechanics [16,17]. The OU process can be thought of as a modification of the random walk, in which the particle is subject to a harmoniclike potential hence, tending to drift toward the mean of the process [17]. It has been used as a minimalist model to describe the dynamics of a wide variety of systems, from volatility in stock markets [18] to vortex pinning in superconductors [19,20] and, more recently, active matter [21–23]. The Brownian motion was the first proposed model of trait evolution [24], and also used as a model of gene frequency evolution [25]. The BM can essentially be viewed as a neutral model (no selection), so evolution happens just by drift. The OU process was introduced as an alternative to the physical BM and already has a long-standing contribution to evolutionary biology. The standard OU process, like BM, assumes random drift but also incorporates stabilizing selection, i.e., whereby a trait is attracted to a selection optimum. More

*Corresponding author: paulo.acampos@ufpe.br

recently, the OU process [26] has proved to be accurate to studies of gene-expression evolution in Drosophila [27], as well as in mammalian species [28]. These quantitative genetics approaches have also been used to study drug-exposed populations of cancer cells to infer persister probability [29], as well as the role of gene expression noise on adaptation and evolution of drugresistance [30].

The current contribution of this work relies on a phenotypic trait evolution model which incorporates explicitly phenotypic plasticity and environmental change into the conventional OU model. In particular, we address a major problem in quantitative genetics which is poorly understood, namely, the observation of skewness in distributions of phenotypic traits. These observations are not captured by the standard OU model. We show that the combined effect of phenotypic plasticity and environmental change can lead to considerably skewed trait distributions. Additionally, we study the conditions that can lead populations to persistence or extinction upon changing the rate of environmental change.

II. PHENOTYPIC EVOLUTION TOWARDS A MOVING OPTIMUM

In the context of phenotypic evolution, the OU stochastic differential equation describing the change in a given trait x is described by

$$dx(t) = \sigma dB(t) + \alpha(\theta - x(t))dt, \tag{1}$$

where $dB(t)$ is a Wiener process of variance one and null mean which models the Brownian motion. From now on, we will set $\sigma = 1$, so it is implicit that all other quantities are expressed in units of σ. The parameter α determines the strength of selection toward the optimal expression level of the trait θ [31]. Therefore, the model assumes stabilizing selection [32], and since then it has been used to infer the extent of stabilizing and convergent evolution of evolving expression levels [27,28,33].

The probability distribution function (PDF), $P(x,t)$, of an OU process evolves towards the stationary Boltzmann distribution $P(x) = \sqrt{\alpha/\pi\sigma^2}e^{-2V(x)/\sigma^2}$, where $V(x) = \frac{1}{2}\alpha(x-\theta)^2$ makes the role of an effective potential associated to the deterministic force of selection $F(x) = -V'(x) = -\alpha(x-\theta)$ [see Fig. 1(a)]. The stationary probability density of phenotypic trait values are normally distributed with mean θ and variance $\sigma^2/2\alpha$. In fact, quantitative genetics makes use of the assumption of normality as a null model [34].

Here we propose modifications of the conventional Ornstein-Uhlenbeck which account for (i) continuous change of the environmental conditions leading to a time-dependent phenotypic optimum $\theta(t)$, and (ii) phenotypic plasticity. For assumption (i), we assume that environmental variations result in the change of the phenotypic optimum, which in its turn varies linearly with time, i.e., $\theta(t) = vt$, where v defines the rate of environmental change [3]. By substituting $\theta(t)$ into Eq. (1) and transforming to the reference frame moving with θ, it now becomes clear that $y = x - \theta$ also follows a conventional OU process,

$$dy = -\alpha(y + v/\alpha)dt + dB, \tag{2}$$

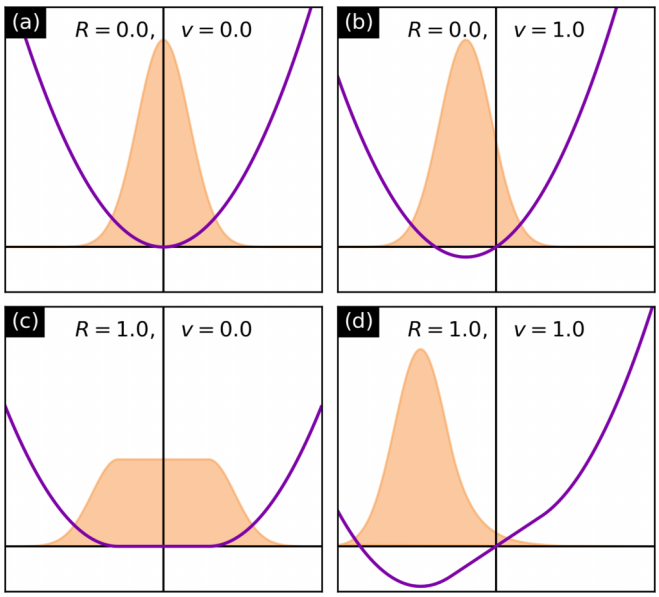

FIG. 1. Schematic plots of the effective potential (lines) and the stationary probability densities (filled curves) for (a) no plasticity and static optimum, (b) no plasticity and moving optimum, (c) phenotypic plasticity R and static optimum, and (d) phenotypic plasticity R and moving optimum. The horizontal axis corresponds to trait values with respect to the optimum, indicated by the vertical line. In all cases, the strength of selection is set at $\alpha = 1.5$.

with a steady optimum at $-v/\alpha$ for the variable y. Equation (2) can be viewed as the equation of a Brownian particle subjected to the tilted harmonic potential $\tilde{V}(y) = \frac{1}{2}\alpha y^2 + vy$. Accordingly, the steady-state phenotypic trait distribution is also Gaussian,

$$P(y) = \frac{\alpha}{\sqrt{\pi\sigma^2}}e^{-(\alpha y^2 + 2vy)/\sigma^2}, \tag{3}$$

but now the most probable trait is lagged, v/α behind the optimum value, see Fig. 1(b). This way, environmental variation results in a steady phenotypic lag which will determine the population's adaptation level. A higher pace will result in lower adaptation and, at some point, can compromise population persistence [3].

III. COMBINED EFFECT OF A MOVING OPTIMUM AND PHENOTYPIC PLASTICITY

Although widespread, the plastic response can not be unrestrained. Otherwise, organisms would always exhibit the best-adapted trait for a given environmental condition, and the population risk of extinction would no longer be a concern. The limits and costs of plasticity are commonly related to the energy and molecular material needed to anticipate environmental variation leading to the most applicable phenotypic response [35]. Furthermore, strong phenotypic plasticity can limit the potential evolutionary responses owing to the inherent costs of plasticity, but mainly because of lower standing genetic variation [36]. For instance, a recent study of the African savannah butterfly Bicyclus anynana in seasonal environments found that the potential for evolutionary change in plasticity is constrained by the lack of standing genetic

variation [7]. Besides, it is also alleged that strong phenotypic plasticity can enhance extinction probability in more unpredictable environments [37]. Thus, it is crucial to understand how plasticity and selection can interact.

To account for phenotypic plasticity, we first define the reaction norm, an array of phenotypes that will be developed by a genotype across a variety of different environmental conditions [38,39]. In short, the reaction norm describes the sensitivity of an organism with a given genome to some environmental variable, and can be represented as a curve that relates, the contribution of environmental variation to observed phenotypic variation. Here we will assume that a linear reaction norm holds over a limited range, $|x-\theta| < R$, thus inflicting limits to the plastic response, which certainly adds realism to the modeling of plasticity [40]. The resulting phenotype matches the environment in this range, and the fitness is maximum. We neglect any time lag between environmental variation and phenotypic response [35]. Under this new perspective, the walker (variable x) now defines the center of this tolerance range, and so when $|x-\theta| \leqslant R$, the particle is under free Brownian motion as the deterministic component of the OU process vanishes. On the other hand, when $|x-\theta| > R$, the stabilizing force that reads $-\alpha[x-\theta-\mathrm{sgn}(x-\theta)R]$, comes into action. Under the reasoning of Lande's model [32], x can be devised as the elevation of the reaction norm, i.e., it provides the genetic additive effect in the reference environment $\theta = 0$. Yet, the plastic component equals $(\theta - x)$ when $|x-\theta| < R$, or $\pm R$ when $|x-\theta| > R$. By establishing a range of validity of the linear reaction norm, as done here, one avoids some spurious outcomes in the case of the unbounded limit of the plastic component, such as the dominance of the relative contribution of that component to the phenotype, approaching one as the optimum phenotype $\theta(t)$ moves further from the reference environment $\theta = 0$, whereas the contribution from the genetic counterpart shrinks [41].

Once again, changing to the frame moving with the optimum, $y = x - vt$ is described by the following equation

$$dy = -\frac{\partial}{\partial y}[V(y) + vy]dt + dB, \tag{4}$$

where

$$V(y) = \begin{cases} 0, & \text{if } |y| < R, \\ \frac{1}{2}\alpha(y - \mathrm{sgn}(y)R)^2, & \text{if } |y| > R. \end{cases} \tag{5}$$

Since the deterministic part of Eq. (4) can still be derived from a time independent potential, once again the stationary PDF follows the Boltzmann distribution,

$$P(y) = \frac{e^{-2[V(y)+vy]/\sigma^2}}{\int dy\, e^{-2[V(y)+vy]/\sigma^2}}. \tag{6}$$

Plots of $V(y)$ and $P(y)$ with plasticity $R = 1.0$ are shown in Fig. 1(c), for $v = 0$, and Fig. 1(d), for $v = 1.0$. Notice that plasticity induces a larger lag of the most probable trait value, given by $R + v/\alpha$, as compared to the nonplastic case. In addition, now the distribution is no longer Gaussian and becomes considerably skewed for $v > 0$. Figure 2 depicts the skewness and mean population fitness (relative to the optimum), which we define as the expected value $\bar{W}_{\mathrm{opt}} = \int dy[-V(y)]P(y)$.

Notice that Eqs. (4) and (6) reduce respectively to Eqs. (2) and (3) in the limit $R = 0$. Another interesting limit is that of large α, for which case the effective potential can be approximated by an infinitely deep square well and the stationary PDF simplifies to a truncated exponential distribution: $P(y) = ve^{-2vy/\sigma^2}/[\sigma^2 \sinh(2vR/\sigma^2)]$, for $|y| < R$, and $P(y) = 0$ otherwise. The dashes in Fig. 2 correspond to the skewness calculated for this distribution. In fact, under plasticity, the distribution $P(y)$ describes the distribution of breeding values (genetic component) of the phenotype. Note that both the rate of environmental variation and strength of selection play a significant role in shaping the phenotypic distribution at stationarity. We also observe that deviation from normality occurs at larger α for larger rates of environmental change v. Still, larger v at the strong selection regime can result in more significant skewness. Assuming a density-independent population growth, the population declines in size when the mean population fitness $\bar{W} < 1$ [or equivalently, the per capita population growth rate $\ln(\bar{W}) < 0$, as used for continuous time models], which is defined up to an additive constant: $\bar{W} = W_{\mathrm{max}} + \bar{W}_{\mathrm{opt}}$, with W_{max} denoting the fitness of the optimum phenotype. In Fig. 3, we show the critical rate of environmental change, v_c, beyond which the population goes extinct. To account for the cost of plasticity, a cost function $C(R)$ is included to the definition of the mean fitness

$$\bar{W} = W_{\mathrm{max}} - C(R) + \int dy[-V(y)]P(y). \tag{7}$$

By choosing the cost function to depend on R, we assume that the cost of plasticity is associated with the maintenance of the sensory and regulatory machinery needed for plasticity [35]. In an experimental study, a quadratic form for the cost function was suggested [42]. Besides, the quadratic form

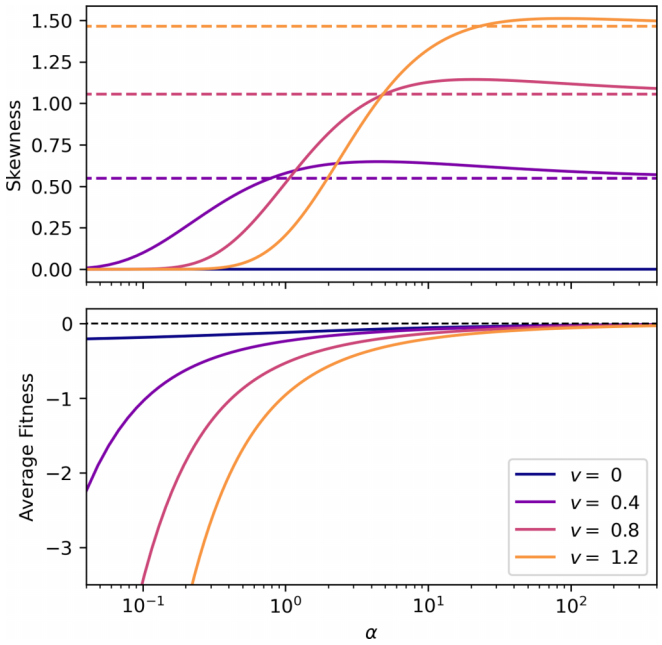

FIG. 2. Skewness (upper panel) and mean population fitness relative to the optimum (lower panel) as a function of the strength of selection α. The other parameter values are phenotypic plasticity $R = 1.0$, and the rates of environmental change, v, are indicated in the legends. Dashed lines correspond to the analytical approximation for the large-α limit.

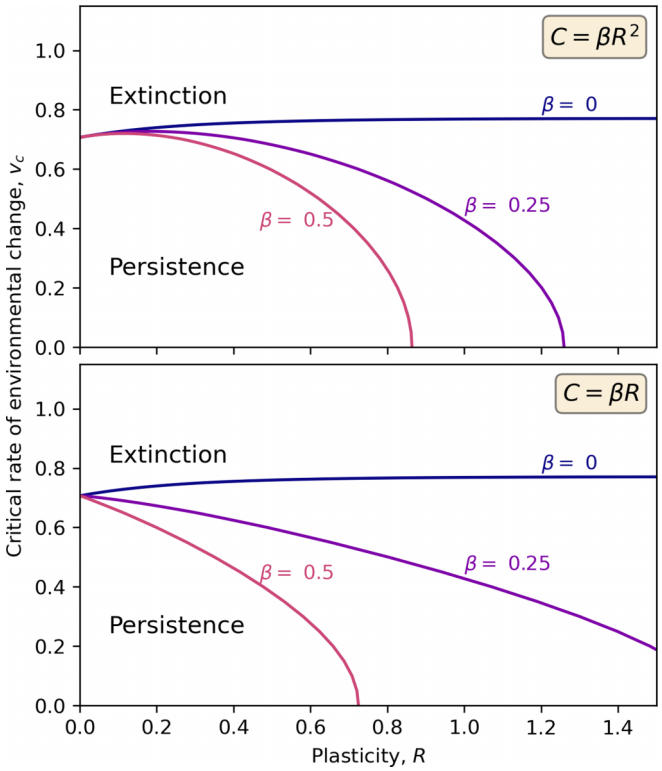

FIG. 3. Critical rate of environmental change, v_c, as a function of phenotypic plasticity, R. The lines delimitate the domains of population persistence and extinction. Results are shown for two different models of the cost of plasticity, quadratic (top) and linear (bottom), and different values of the cost coefficient β. In all cases, $\alpha = 1.0$ and $W_{\max} = 1.5$.

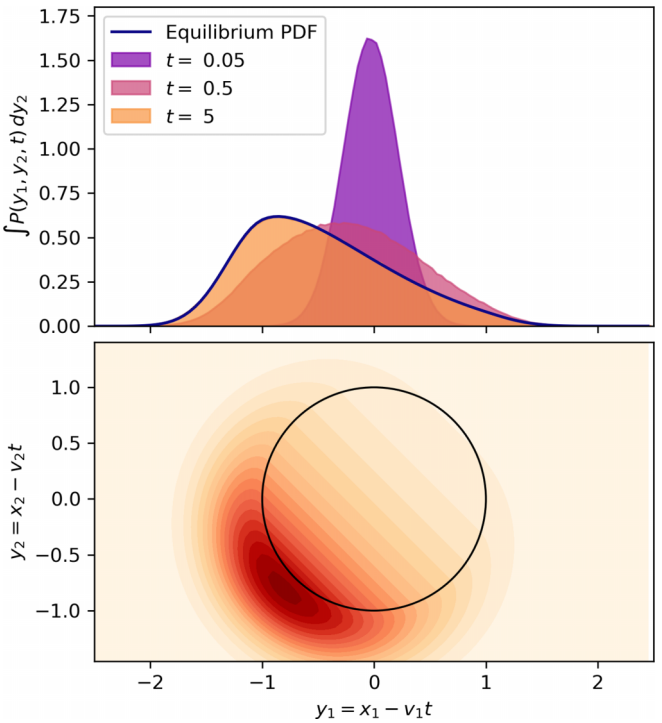

FIG. 4. Upper panel: reduced probability density of trait X_1 around the phenotypic optimum at different times and at stationarity, $P(y_1, t)$, with $y_1 = x_1 - v_1 t$. Lower panel: Joint probability density of traits X_1 and X_2 around the phenotypic optimum at stationarity, $P(y_1, y_2)$, with $y_1 = x_1 - v_1 t$ and $y_2 = x_2 - v_2 t$. The circle delimits the area around the phenotypic optimum within a radius R. In the plot, $v_1 = v_2 = 0.5$ and $\alpha = 5.0$.

for the cost function, $C = \beta R^2$, a linear function, $C = \beta R$, is here considered, where β is a constant. As we see, the scenario in both cases is qualitatively similar. The boundaries between persistence and extinction phases of the population for different values of β are shown. Our results unveil a striking feature: the existence of an upper bound for the critical rate of environmental variation. In the plot, we observe that for $v \geqslant 0.8$, the population can no longer persist, even for a null cost of plasticity. The ideas above can be extended straightforwardly for the case of multiple traits. Instead of a phenotypic range, as defined for the one-dimensional case, now the plasticity R corresponds to the radius of a hypersphere in the trait space, which comprises all traits x_k. Once again, their contributions to fitness are determined by the distance to their respective optima, $y_k = x_k - \theta_k$. Moreover, we assume that the optimum of each trait k drifts at a constant rate, that is, $\theta_k = v_k t$. Therefore, in analogy to Eq. (4), we model the time evolution of the N variables y_k by the following vector equation

$$d\boldsymbol{r} = -\nabla[V(\boldsymbol{r}) + \boldsymbol{v}\cdot\boldsymbol{r}]dt + d\boldsymbol{B}, \tag{8}$$

where $\boldsymbol{r} = (y_1, y_2, \ldots, y_N)$, $\nabla = (\frac{\partial}{\partial y_1}, \frac{\partial}{\partial y_2}, \ldots, \frac{\partial}{\partial y_N})$, $\boldsymbol{v} = (v_1, v_2, \ldots, v_N)$, and

$$V(\boldsymbol{r}) = \begin{cases} 0, & \text{if } |\boldsymbol{r}| < R, \\ \frac{1}{2}\alpha\left(\boldsymbol{r} - \frac{\boldsymbol{r}}{|\boldsymbol{r}|}R\right)^2, & \text{if } |\boldsymbol{r}| > R. \end{cases} \tag{9}$$

Since the deterministic part of Eq. (8) can be expressed as the gradient of an effective potential, the corresponding Fokker-Planck equation admits a stationary solution, given once more by the Boltzmann distribution. Figure 4 displays both the joint probability density of $y_1 = x_1 - v_1 t$ and $y_2 = x_2 - v_2 t$, $P(y_1, y_2)$, and the reduced probability density of y_1, which equals $P(y_1) = \int_{-\infty}^{\infty} P(y_1, y_2) dy_2$. In the plot $v_1 = v_2 = v$. The results are qualitatively the same as those seen for a single trait. We observe that both distributions are highly skewed concomitantly with a considerable phenotypic lag in both directions. If, for instance, we had $v_1 = 0$ and $v_2 = v$, y_1 would become normally distributed, whereas the distribution of y_2 would be skewed (data not shown). In this way, the shape of the joint probability density and the reduced probability density are influenced not only by the magnitude of $\boldsymbol{v}$ but also by its direction. Moreover, the joint probability density displays a strong correlation between the traits. As shown in Fig. 5, these results from the combination of plasticity and the continued change of the phenotypic optimum in both directions.

IV. DISCUSSIONS AND CONCLUSIONS

Here we have investigated phenotypic evolution within the framework of the Ornstein-Uhlenbeck process. Our main goal is to use this framework to address the role of environmental variation and phenotypic plasticity in the evolutionary pro-

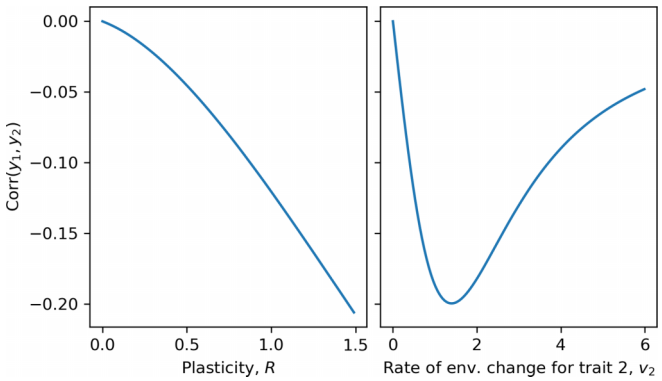

FIG. 5. Correlation between traits y_1 and y_2 for the same situation as in Fig. 4, but: (Left) with varying R and fixed $v_1 = v_2 = 0.5$; (Right) with varying v_2 and fixed $R = 1$, $v_1 = 0.5$. Notice that Corr(y_1, y_2) becomes significant when one increases plasticity and the rates v_1, v_2, thus suggesting that this quantity can be used as a signature of the interplay between plasticity and environmental change rate. For large v_2 the correlation tends to shrink because v_1 becomes negligible in comparison to v_2.

cess. It is of considerable interest to understand how natural selection and other evolutionary forces combine to change the phenotypic spectrum. The assumption that phenotypic traits are normally distributed is a fundamental premise in quantitative genetics [43]. One expects skewed phenotypic distribution to affect the evolutionary process. Deviations from normality can, for instance, break down the linearity of the parent-offspring regression used as a central tool to measure the heritability of phenotypic traits [34]. Deviations from the normality assumption are found for juvenile body size of bird species [34], contemporary human traits [44], and avian breeding phenology in wild bird populations [45], among others. Among the processes that are pointed out as possible explanations for the departure from the normality assumption are strong directional selection, migration between heterogeneous populations with respect to their adaptive optimum, and skewed stabilizing selection [45].

The modification of the standard Ornstein-Uhlenbeck (OU) process by considering a continued directional shift of the phenotypic optimum in time supplies the modeling with a combination of stabilizing and directional selection, such as verified in contemporary human traits [44]. We show that under the framework of the OU process, the assumption of a moving optimum results in a phenotypic lag that equals v/α, i.e., increases with the rate of environmental change and decreases with the strength of selection. However, the sustained displacement of the phenotypic optimum does not account for any deviation from the normality assumption. We demonstrate that, in the context of the OU model, where the stabilizing force is a linear function of trait, deviations from the normality assumption require the existence of phenotypic plasticity, but only the common occurrence of both a moving optimum and phenotypic plasticity can explain the appearance of skewed trait distributions. Of course, a skewed distribution can also be obtained by considering a model where the stabilizing force is nonlinear from the very beginning. However, such a procedure would miss the simplicity of the OU model and the opportunity of systematically investigating the effect of phenotype plasticity, both present in our modeling. Our results reveal the need for a more accurate analysis of empirical evidence of the processes or their absence through the inference from the skewness of empirical phenotypic distributions under different conditions.

The postulation of either a moving optimum or phenotypic plasticity gives rise to an effective potential or, equivalently, to an effective fitness landscape. A distortion of the original harmoniclike potential is seen in the presence of phenotypic plasticity. The common occurrence of a moving optimum and phenotypic plasticity gives rise to a skewed effective potential, which explains the observed asymmetry in the distribution of trait values. We have obtained a phase diagram encircling the domain of population extinction and persistence. An important evolutionary consequence of our predictions is the existence of an upper bound for the critical rate of environmental change v_c even when there is no cost of plasticity $\beta = 0$. This outcome is at odds with previous findings that display an accelerating rate of growth of the critical rate of environmental change with plasticity [3,46], and the critical rate v_c grows with no bound, which sounds unrealistic. Our modeling avoids the spurious effect of the dominance of the plastic component to the phenotype [41]. In Ref. [46], an upper bound for v_c is found but under the assumption of a decelerating rate of environmental variation.

ACKNOWLEDGMENTS

P.R.A.C. and C.C.S.S. are partially supported by Conselho Nacional de Desenvolvimento Científico e Tecnológico (CNPq) under Grant No. 301795/2022-3 and No. 312240/2021-0. P.R.A.C. and C.C.S.S. also acknowledge financial support from Coordenação de Aperfeiçoamento de Pessoal de Nível Superior (CAPES) (Project No. 0041/2022). P.R.A.C. acknowledges Universidade Federal de Pernambuco Edital Produção Qualificada. D.C. is supported by Conselho Nacional de Desenvolvimento Científico e Tecnológico (CNPq), while O.F. is supported by Fundação de Amparo à Ciência e Tecnologia do Estado de Pernambuco (FACEPE).

[1] D. Nogués-Bravo, F. Rodríguez-Sánchez, L. Orsini, E. de Boer, R. Jansson, H. Morlon, D. A. Fordham, and S. T. Jackson, Cracking the code of biodiversity responses to past climate change, Trends Ecol. Evol. **33**, 765 (2018).

[2] P.-O. Cheptou, A. L. Hargreaves, D. Bonte, and H. Jacquemyn, Adaptation to fragmentation: evolutionary dynamics driven by human influences, Philos. Trans. R. Soc., B **372**, 20160037 (2017).

[3] L.-M. Chevin, R. Lande, and G. M. Mace, Adaptation, plasticity, and extinction in a changing environment: towards a predictive theory, PLoS Biol. **8**, e1000357 (2010).

[4] D. J. Futuyma, Evolutionary biology today and the call for an extended synthesis, Interface Focus. **7**, 20160145 (2017).

[5] K. N. Laland, T. Uller, M. W. Feldman, K. Sterelny, G. B. Müller, A. Moczek, E. Jablonka, and J. Odling-Smee, The extended evolutionary synthesis: its structure, assumptions and predictions, Proc. R. Soc. B **282**, 20151019 (2015).

[6] A. A. Agrawal, Phenotypic plasticity in the interactions and evolution of species, Science **294**, 321 (2001).

[7] V. Oostra, M. Saastamoinen, B. J. Zwaan, and C. W. Wheat, Strong phenotypic plasticity limits potential for evolutionary responses to climate change, Nat. Commun. **9**, 1005 (2018).

[8] R. B. Huey, M. R. Kearney, A. Krockenberger, J. A. Holtum, M. Jess, and S. E. Williams, Predicting organismal vulnerability to climate warming: roles of behaviour, physiology and adaptation, Philos. Trans. R. Soc., B **367**, 1665 (2012).

[9] A. Sentis, J. Morisson, and D. S. Boukal, Thermal acclimation modulates the impacts of temperature and enrichment on trophic interaction strengths and population dynamics, Global Change Biology **21**, 3290 (2015).

[10] B. Gilbert, T. D. Tunney, K. S. McCann, J. P. DeLong, D. A. Vasseur, V. Savage, J. B. Shurin, A. I. Dell, B. T. Barton, C. D. Harley *et al.*, A bioenergetic framework for the temperature dependence of trophic interactions, Ecol. Lett. **17**, 902 (2014).

[11] S. E. Gilman, M. C. Urban, J. Tewksbury, G. W. Gilchrist, and R. D. Holt, A framework for community interactions under climate change, Trends Ecol. Evol. **25**, 325 (2010).

[12] E. Post and C. Pedersen, Opposing plant community responses to warming with and without herbivores, Proc. Natl. Acad. Sci. USA **105**, 12353 (2008).

[13] B. T. Barton and O. J. Schmitz, Experimental warming transforms multiple predator effects in a grassland food web, Ecol. Lett. **12**, 1317 (2009).

[14] A. Sentis, R. Bertram, N. Dardenne, F. Ramon-Portugal, I. Louit, G. Le Trionnaire, J.-C. Simon, A. Magro, B. Pujol, J.-L. Hemptinne *et al.*, Different phenotypic plastic responses to predators observed among aphid lineages specialized on different host plants, Sci. Rep. **9**, 1 (2019).

[15] P. Kratina, H. S. Greig, P. L. Thompson, T. S. Carvalho-Pereira, and J. B. Shurin, Warming modifies trophic cascades and eutrophication in experimental freshwater communities, Ecology **93**, 1421 (2012).

[16] L. Reichl, *A Modern Course in Statistical Physics* (Wiley, New, 1998).

[17] N. G. Van Kampen, *Stochastic Processes in Physics and Chemistry*, Vol. 1 (Elsevier, Amsterdam, 1992).

[18] E. M. Stein and J. C. Stein, Stock price distributions with stochastic volatility: an analytic approach, Rev. Financ. Stud. **4**, 727 (1991).

[19] M. W. Coffey and J. R. Clem, Unified theory of effects of vortex pinning and flux creep upon the rf surface impedance of type-II superconductors, Phys. Rev. Lett. **67**, 386 (1991).

[20] B. Raes, J. Van de Vondel, A. V. Silhanek, C. C. de Souza Silva, J. Gutierrez, R. B. G. Kramer, and V. V. Moshchalkov, Local mapping of dissipative vortex motion, Phys. Rev. B **86**, 064522 (2012).

[21] E. Fodor, C. Nardini, M. E. Cates, J. Tailleur, P. Visco, and F. van Wijland, How Far from Equilibrium Is Active Matter? Phys. Rev. Lett. **117**, 038103 (2016).

[22] L. L. Bonilla, Active ornstein-uhlenbeck particles, Phys. Rev. E **100**, 022601 (2019).

[23] D. Martin, J. O'Byrne, M. E. Cates, E. Fodor, C. Nardini, J. Tailleur, and F. van Wijland, Statistical mechanics of active ornstein-uhlenbeck particles, Phys. Rev. E **103**, 032607 (2021).

[24] J. Felsenstein, Maximum-likelihood estimation of evolutionary trees from continuous characters, Am. J. Hum. Genet. **25**, 471 (1973).

[25] L. L. Cavalli-Sforza and A. W. Edwards, Phylogenetic analysis. models and estimation procedures, Am. J. Hum. Genet. **19**, 233 (1967).

[26] G. E. Uhlenbeck and L. S. Ornstein, On the theory of the brownian motion, Phys. Rev. **36**, 823 (1930).

[27] T. Bedford and D. L. Hartl, Optimization of gene expression by natural selection, Proc. Natl. Acad. Sci. USA **106**, 1133 (2009).

[28] J. Chen, R. Swofford, J. Johnson, B. B. Cummings, N. Rogel, K. Lindblad-Toh, W. Haerty, F. Di Palma, and A. Regev, A quantitative framework for characterizing the evolutionary history of mammalian gene expression, Genome Res. **29**, 53 (2019).

[29] D. A. Kessler and H. Levine, Phenomenological Approach to Cancer Cell Persistence, Phys. Rev. Lett. **129**, 108101 (2022).

[30] D. A. Charlebois, N. Abdennur, and M. Kaern, Gene Expression Noise Facilitates Adaptation and Drug Resistance Independently of Mutation, Phys. Rev. Lett. **107**, 218101 (2011).

[31] T. F. Hansen, Stabilizing selection and the comparative analysis of adaptation, Evolution **51**, 1341 (1997).

[32] R. Lande, Natural selection and random genetic drift in phenotypic evolution, Evolution, **30** 314 (1976).

[33] A. T. Kalinka, K. M. Varga, D. T. Gerrard, S. Preibisch, D. L. Corcoran, J. Jarrells, U. Ohler, C. M. Bergman, and P. Tomancak, Gene expression divergence recapitulates the developmental hourglass model, Nature (London) **468**, 811 (2010).

[34] J. L. Pick, H. E. Lemon, C. E. Thomson, and J. D. Hadfield, Decomposing phenotypic skew and its effects on the predicted response to strong selection, Nat. Ecol. Evol. **6**, 774 (2022).

[35] T. J. DeWitt, A. Sih, and D. S. Wilson, Costs and limits of phenotypic plasticity, Trends Ecol. Evol. **13**, 77 (1998).

[36] C. J. Murren, J. R. Auld, H. Callahan, C. K. Ghalambor, C. A. Handelsman, M. A. Heskel, J. Kingsolver, H. J. Maclean, J. Masel, H. Maughan *et al.*, Constraints on the evolution of phenotypic plasticity: limits and costs of phenotype and plasticity, Heredity **115**, 293 (2015).

[37] T. E. Reed, R. S. Waples, D. E. Schindler, J. J. Hard, and M. T. Kinnison, Phenotypic plasticity and population viability: the importance of environmental predictability, Proc. R. Soc. B **277**, 3391 (2010).

[38] M. Lynch, B. Walsh *et al.*, *Genetics and Analysis of Quantitative Traits*, Vol. 1 (Sinauer Sunderland, MA, 1998).

[39] S. Via, R. Gomulkiewicz, G. De Jong, S. M. Scheiner, C. D. Schlichting, and P. H. Van Tienderen, Adaptive phenotypic plasticity: consensus and controversy, Trends Ecol. Evol. **10**, 212 (1995).

[40] A. Wiesenthal, C. Müller, and J.-P. Hildebrandt, Potential modes of range shifts in euryhaline snails from the baltic sea and fresh water lakes in northern germany, Hydrobiologia **811**, 339 (2018).

[41] S. M. Scheiner, M. Barfield, and R. D. Holt, The genetics of phenotypic plasticity. XVII. response to climate change, Evolutionary Applications **13**, 388 (2020).

[42] J. M. Dechaine, J. A. Johnston, M. T. Brock, and C. Weinig, Constraints on the evolution of adaptive plasticity: costs of plasticity to density are expressed in segregating progenies, New Phytologist **176**, 874 (2007).

[43] D. Falconer and T. Mackay, *Introduction to Quantitative Genetics* (Longman, New York, 1996).

[44] J. S. Sanjak, J. Sidorenko, M. R. Robinson, K. R. Thornton, and P. M. Visscher, Evidence of directional and stabilizing selection in contemporary humans, Proc. Natl. Acad. Sci. USA **115**, 151 (2018).

[45] S. Bonamour, C. Teplitsky, A. Charmantier, P.-A. Crochet, and L.-M. Chevin, Selection on skewed characters and the paradox of stasis, Evolution **71**, 2703 (2017).

[46] P. B. Greenspoon and H. G. Spencer, Avoiding extinction under nonlinear environmental change: models of evolutionary rescue with plasticity, Bio. Lett. **17**, 20210459 (2021).